Journal of Ceramic Processing Research. Vol. 27, No. 1, pp. 141~149 (2026)
(Received 7 November 2025, Received in revised form 15 December 2025, Accepted 24 December 2025)
https://doi.org/10.36410/jcpr.2026.27.1.141

J O U R N A L O F
Ceramic Processing Research

Cytocompatibility and bacterial resistance of polished *versus* glazed partially stabilized zirconia and lithium disilicate ceramics for dental applications

Min-Gu Cho, Youngchae Cho and Deuk Yong Lee*
Department of R&D Center, Hass Co., Ltd., 60, Haan-ro, Gwangmyeong 14322, Korea

Polished or glazed 4 mol% yttria-partially stabilized zirconia (4Y-PSZ) and lithium disilicate (LD) dental ceramics are of considerable importance for intraoral use, as they have a major impact on the cytocompatibility and antibiofilm resistance. In this study, two glazes were applied–that is, Arte (Hass Co., Ltd., Gangneung, Gangwon State, Republic of Korea) and Insync (Jensen Dental, North Haven, CT, USA). Subsequently, the human gingival fibroblast (HGF-1) response and biofilm formation of polished *versus* glazed 4Y-PSZ and LD ceramics were evaluated. For the glazed 4Y-PSZ and LD samples, a low bulk density and water contact angle, essential for biological performance, were evident. Moreover, the viability of the HGF-1 cells was greater than 98% in all samples. The highest cell densities were observed on the Arte-glazed 4Y-PSZ and LD ceramics. Conversely, the Arte-glazed 4Y-PSZ and Insync-glazed LD specimens exhibited the lowest biothickness. The Insync-glazed 4Y-PSZ and Arte-glazed LD samples exhibited the lowest biofilm biomass, indicating improved bacterial resistance compared to the polished samples. Although polishing may be clinically useful as it improves the cell response and reduces biofilm formation, glazing exhibited superior efficacy regardless of the glaze type.

Keywords: Lithium disilicate, Zirconia, Glaze, Cytocompatibility, Biofilm.

Introduction

Today, all-ceramic restorations are widely used as the preferred dental material instead of metal in clinical applications ranging from single-tooth implants to crowns and bridges [1–6]. Transformation-toughened zirconia (ZrO_2), which exhibits excellent mechanical properties—such as strength and fracture toughness—is clinically used in femoral heads of hip joints and dental abutments [7–9]. However, ZrO_2 has been reported to be less aesthetically pleasing than glass ceramics owing to its whiteness and opacity [1, 10]. Glass ceramics are widely used in odontology due to their ability to mimic tooth color, as well as their excellent biocompatibility and mechanical properties, and thermal expansion similar to that of human teeth [1–5]. Of all the ceramics used in dentistry, lithium-based glass ceramics are the most commonly used due to their excellent aesthetics, opalescence, fluorescence, and machinability [5]. Lithium disilicate (LD; $Li_2Si_2O_5$) glass ceramics have a lower strength (350–450 MPa) than that of ZrO_2 but are less prone to chipping and edge fracture than zirconia and have a natural tooth-like appearance [1–5]. Moreover, LD is preferred in the dental field due to its shorter working time and excellent aesthetics [1–6].

Cho et al. [11] argued that surface treatments—such as machining, polishing, and glazing—played a crucial role in improving the wettability, cytocompatibility, and antibiofilm resistance of dental ceramics. Among surface treatments, machined surfaces are not clinically suitable for oral use without polishing or glazing. They reported that polishing reduced the average roughness (*Ra*), whereas glazing created better conditions for cell survival and growth [11]. Consequently, glazed dental crowns are the most widely used clinically. Both polishing and glazing primarily contribute to improving the cytocompatibility and bacterial resistance of oral implant biomaterials [1, 2, 5, 11–15]. Polished ceramics reduce roughness and increase hydrophobicity, promoting protein adsorption and bacteria adhesion [11–15]. Conversely, glazing increases hydrophilicity and reduces protein adsorption, regardless of roughness [14]. As shown in Fig. 1, 4mol% yttria-partially stabilized ZrO_2 (4Y–PSZ, UNC International Co., Ltd., Seoul, Republic of Korea) and LD blocks are clinically used in dental abutments and crowns, respectively [1–6, 9, 11, 16].

Notably, Amber® Mill Abut–Crown (AMA, Hass Co., Ltd., Gangneung, Republic of Korea) is commercially available as a monolithic ceramic block (Fig. 1). It consists of a titanium abutment and link, ZrO_2 ceramic coping, LD glass ceramic, and leucite ceramic for the hole keeper [11]. Previous studies have shown that Insync (Jensen Dental, North Haven, Connecticut, USA)-glazed 4Y–PSZ and AMA (LD) samples exhibited superior human gingival fibroblast (HGF–1, NCTC Clone 929, ATCC, Manassas, VA, USA) and L–929 (Korea

*Corresponding author:
Tel : +82-2020831365
Fax: +82-2020831366
E-mail: duke1208@gmail.com

Fig. 1. Photographs of the 4Y–PSZ and AMA.

Cell Line Bank, Seoul, Republic of Korea) fibroblast attachment and proliferation, improved soft tissue sealing around the dental implants, and reduced biofilm biomass compared to the polished samples [11]. However, no study has compared Arte-glaze specimens (Hass Co., Ltd.) with other specimens.

In this study, the cytocompatibility and bacterial resistance of two types of specimens (4Y-PSZ and AMA) manufactured through polishing or Arte-glaze treatments were investigated. Experimental data from the Arte-glaze samples were compared with previously published data [11]. The null hypothesis was that the surface treatments (polishing and glazing) did not affect the surface properties, cytocompatibility, and antibiofilm formation of 4Y–PSZ and AMA ceramics.

Experimental

Two types of specimens were studied–that is, 4Y–PSZ (Razor 1100) and AMA samples. The AMA sample was sintered at 840ºC for 15 min using a dental furnace (Austromat 624*i*, Dekema Dental–Keramiköfen GmbH, Freilassing, Germany). The heat-treated ceramic blocks (Fig. 1) were manufactured as discs with a diameter of 12 mm and a thickness of 0.6 mm. The specimens were then ground, polished, and glazed until they reached their final crystalline form. Before glazing, alumina particles (50 μm) were sandblasted using a dental sandblaster (Basic eco, Renfert GmbH, Hilzingen, Germany) at a pressure of 2 bar and an angle of 70° with a spray gap of approximately 10 mm. The spray was maintained for 20 s.

As shown in Fig. 2, the Amber® Arte glaze paste kit or the Insync® stain and glaze paste kit were applied to

Fig. 2. Photographs of the glaze kits: the Amber® Arte and Insync® glaze pastes and liquids.

the specimen surface. After sandblasting and ultrasonic treatment, the sandblasted samples were glazed in a dental furnace at 760–800 ºC for 1 min. After heat treatment, inspection was performed to ensure that the glaze had been applied properly, and if not, the self-glazing and polishing process was repeated [11, 17].

The bulk density (n = 5) and apparent porosity (n = 5) of the 4Y-PSZ and AMA ceramics were examined [11, 17–20]. The WCA (n = 5) was also measured [11, 17–20]. The arithmetic average roughness (*Ra*) of the samples (n = 5) was measured [11]. The experimental procedures have been described in detail in previous work [11, 17–20].

Cytotoxicity (n = 5) was measured based on the International Organization for Standardization (ISO) 10993–5 standard [11, 17–20]. Pellets were extracted aseptically with serum in a single-strength Minimum Essential Medium (1× MEM, Dulbecco's Modified Eagle's Medium (Gibco, Life Technologies Ltd., Paisley, UK) with 10% fetal bovine serum (Gibco) and 1% penicillin–streptomycin (Gibco)). The extraction ratio of pellet to extraction vehicle was 0.2 g/mL (ISO 10993-12) [8, 11, 18–20]. After incubation for 24 h, the test extracts were placed on separate confluent monolayers of HGF-1. Cell proliferation was assayed using the cell counting kit-8 (CCK-8; Dojindo Molecular Technologies, Inc., Tokyo, Japan) [11, 17–20]. Cell viability and proliferation assay procedures have been

Table 1. Type and composition of materials.

Product	Model	Composition	Manufacturer
4Y-PSZ	Razor 1100	4 mol% Y_2O_3–ZrO_2	UNC International, Seoul, Korea
Amber® Mill	Abut–Crown	62.9% SiO_2, 28.1% Li_2O, 1.21% Al_2O_3, 1.47% P_2O_5, etc.	Hass Co., Ltd. Gangneung, Korea
Amber Arte	Arte, glaze paste and liquid	Paste : 55–65% silica, Li_2O, Al_2O_3, B_2O_3, other oxides; liquid: butanediol, glycerin, etc.	Hass Co., Ltd. Gangneung, Korea
Insync	Insync, glaze paste and liquid	paste: silica, cristobalite, quartz, silicon, boron oxide, aluminum oxide, glycerin, calcium oxide, zinc oxide, tin oxide; liquids: <100 1,3-butanediol, <95 glycerin, <90 1,2-propylene glycol, <1% zinc chloride	Jensen Dental, North Haven, USA

well described in previous studies [11, 17–20].

The live/dead cell assay (n = 5) was investigated to evaluate the cell adhesion and proliferation on various surface-treated specimens [11, 18–21]. After 72 h of culture, the proliferative activity of the HGF-1 cells was analyzed with an aid of a live/dead assay kit (Thermo Fisher Scientific, Waltham, MA, USA), with green and red staining indicating the living and dead cells, respectively [11, 18–21]. The live and dead HGF-1 cells were observed using a fluorescence microscope (DP73; Olympus, Tokyo, Japan) [11, 18–20].

To assess the antibiofilm formation, multispecies human salivary biofilm was prepared by collecting human saliva from healthy adult donors without active caries or periodontal disease and who had not taken antibiotics during the previous 3 months [11, 21–24]. This study was conducted in accordance with the Declaration of Helsinki and was approved by the Institutional Review Board of the Yonsei University Dental Hospital (IRB No. 2-2024-0005) [11]. To minimize the influence of oral hygiene and dietary habits, participants were instructed not to brush their teeth for 24 h prior to saliva collection and not to eat for at least 2 h prior. Saliva was collected from 10 participants and mixed in equal proportions to create a mixed saliva sample. This mixed saliva was diluted to a 30% concentration in sterile glycerol and stored at -80 °C for use as a biofilm model. The biofilm model was cultured in a medium containing McBain's medium (type II, porcine, gastric) (2.5 g/L), tryptone (2.0 g/L), bacterial peptone (2.0 g/L), yeast extract (1.0 g/L), NaCl (0.35 g/L), $CaCl_2$ (0.2 g/L), KCl (0.2 g/L), cysteine hydrochloride (0.1 g/L), hemin (0.001 g/L), and vitamin K1 (0.0002 g/L) [11, 21–25]. The sample was inoculated by mixing 1.5 mL of McBain medium and 30 μL of mixed saliva and cultured at 37 °C in a 5% CO_2 environment. The existing medium was removed every 24 h to replace nutrients, and the biofilm was cultured in the same environment for a total of 72 h [11, 23]. The detailed experimental procedure is described elsewhere [11, 21–25]. The biofilm was observed using a confocal laser scanning microscope (LSM980, Carl Zeiss, Thornwood, NY, USA), and the biofilm thickness and biomass were determined using the system's software (Zen, Carl Zeiss, Thornwood, NY, USA), COMSTAT plug-in (Technical University of Denmark, Kongens Lyngby, Denmark), and ImageJ (version 1.54, NIH, Bethesda, MA, USA) software, respectively [11, 21–24].

All statistical analyses were done using IBM SPSS software (version 23.0, IBM Co., Armonk, NY, USA). Two-way analysis of variance (ANOVA) with Tukey's honestly significant difference *post-hoc* test was used for analyzing experimental data. *In-vitro* and *ex-vivo* assays were assayed using one-way ANOVA and Tukey's *post hoc* test. The significance level was set at $p < 0.05$ [11, 18–20].

Result and Discussion

The experimental results of the bulk density and porosity of various samples are shown in Fig. 3. The bulk density of the sample was affected by the material type (partial eta-squared, η_p^2=0.998, $p < 0.001$), surface treatment (η_p^2=0.873, $p < 0.001$), and interaction between the material type and surface treatment (η_p^2=0.766, $p < 0.001$). Tukey's *post-hoc* analysis showed a significant difference between polishing and glazing ($p < 0.001$), and a difference was evident between the Arte and Insync glazes (p = 0.038). Thus, the null hypothesis that the material type and surface treatment did not affect the bulk density of 4Y-PSZ and AMA ceramics was rejected.

Overall, the material type (η_p^2=0.998) had a greater impact on the density than the surface treatment (η_p^2=0.873). As the density of the glaze was lower than that of the bulk sample, which led to a decrease in the density of the glazed sample, the porosity was also measured. The increase in porosity qualitatively indicated that the microstructure of the glazed samples was more loosely bounded than that of the polished samples. The apparent porosity was statistically significant between groups ($p < 0.001$). No significant difference was evident within the groups. The porosity was not affected by the

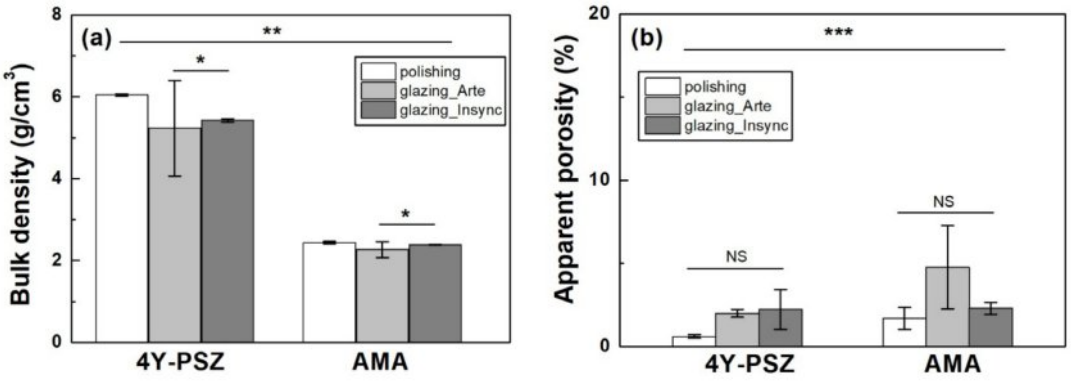

Fig. 3. (a) Bulk density and (b) apparent porosity of various samples. Statistical significance is indicated by * ($p < 0.05$), ** ($p < 0.01$), and *** ($p < 0.001$, n = 5). NS represents statistically not significant.

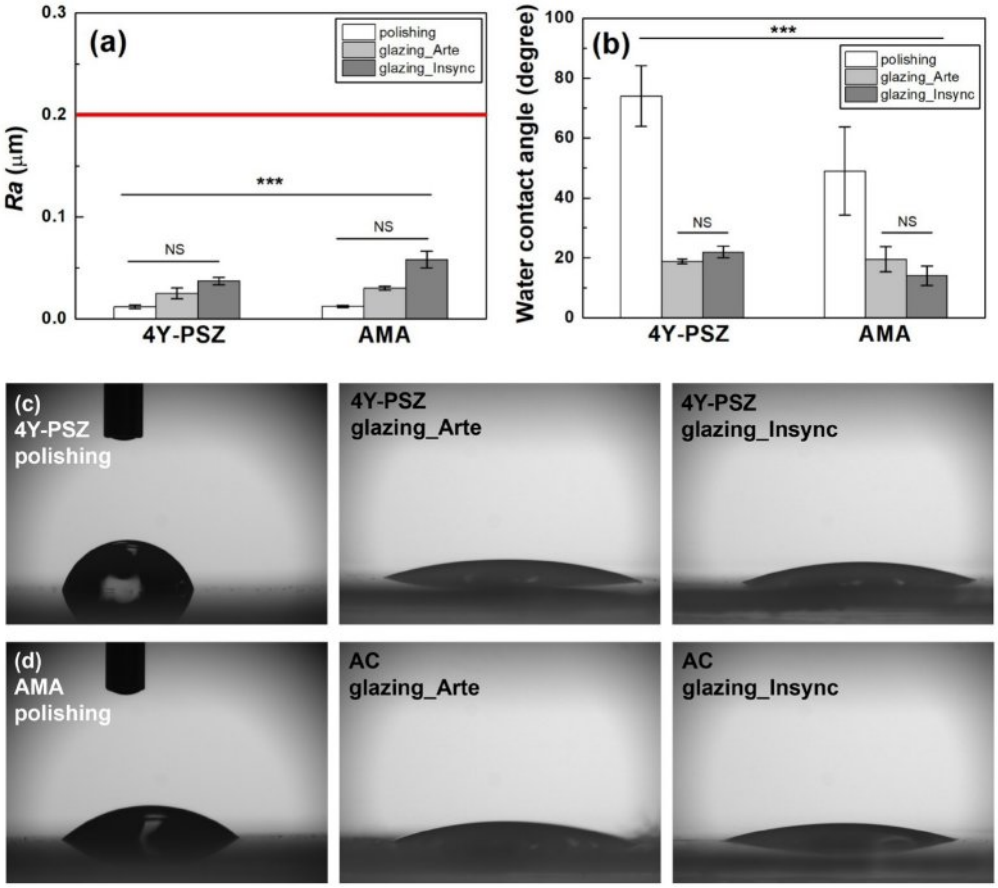

Fig. 4. Changes in (a) *Ra* and (b) WCA of the various samples based on the surface condition. WCA images of the (c) 4Y-PSZ and (d) AMA ceramics with various surface treatments. Statistical significance is indicated by *** ($p < 0.001$, $n = 5$). NS indicates statistically insignificant.

material type (η_p^2=0.104, $p = 0.262$) or surface condition (η_p^2=0.166, $p = 0.335$). Thus, the material type had a greater influence on the bulk density than the surface treatment but polishing and glazing did not affect the product porosity.

The *Ra* of the 4Y-PSZ and AMA samples increased after glazing (Fig. 4(a)). The null hypothesis that the material type did not affect the *Ra* of the 4Y-PSZ and AMA ceramics between groups was rejected ($p < 0.001$). However, the *Ra* of the 4Y-PSZ and AMA dental ceramics was not influenced by the material type (η_p^2=0.128, $p = 0.191$) and surface treatment (η_p^2=0.248, $p = 0.157$) within the group. Moreover, no interaction between the material type and surface treatment (η_p^2=0.248, $p = 0.157$) was evident.

In the clinical study, smooth samples with mirror-like surfaces did not provide any advantage over samples below the roughness threshold (*Ra* = 0.2 μm, red line in Fig. 4(a)), which balances the bacterial adhesion and soft tissue sealing [9, 11, 25, 26]. The samples used in this study had a roughness of less than 0.2 μm (Fig. 4(a)), indicating no significant difference in cytocompatibility and bacterial resistance. Conversely, the impact of roughness was minimal. When the Arte or Insync glaze was applied to polished 4Y-PSZ, the WCA (Figs. 4(b)~(d)) decreased dramatically from 74.0° to 18.8° and 21.9°, respectively, suggesting a significant increase in the hydrophilicity of 4Y-PSZ.

Table 2. Cell viability, biofilm biothickness, and biomass of 4Y-PSZ and AMA ceramics.

Product	Surface condition	Cell viability (%)	Biothickness (μm)	Biomass ($\mu m^3/\mu m^2$)
4Y-PSZ	Polishing	98.9 ± 9.93	85.83±2.887	2.793±1.357
	Glazing_Arte	112.3 ± 9.86	74.16±2.887	14.58±6.300
	Glazing_Insync	110.6 ± 9.87	79.16±3.819	2.408±1.556
Amber® Mill	Polishing	107.7 ± 11.36	89.25±1.750	1.775±0.920
Abut-Crown	Glazing_Arte	117.9 ± 13.7	85.75±3.500	0.620±0.384
	Glazing_Insync	116.9 ± 10.64	72.33±8.808	1.233±0.025

A similar trend was evident in the AMA specimens. The WCA was reduced by the material type (η_p^2=0.308, p = 0.017) and surface condition (η_p^2=0.882, p < 0.001), and the interaction between the material type and surface condition (η_p^2=0.335, p = 0.038). Consequently, glaze treatment was found to have a greater effect on the WCA of the 4Y-PSZ and AMA ceramics. In all samples, the WCA significantly decreased after the glazing treatment.

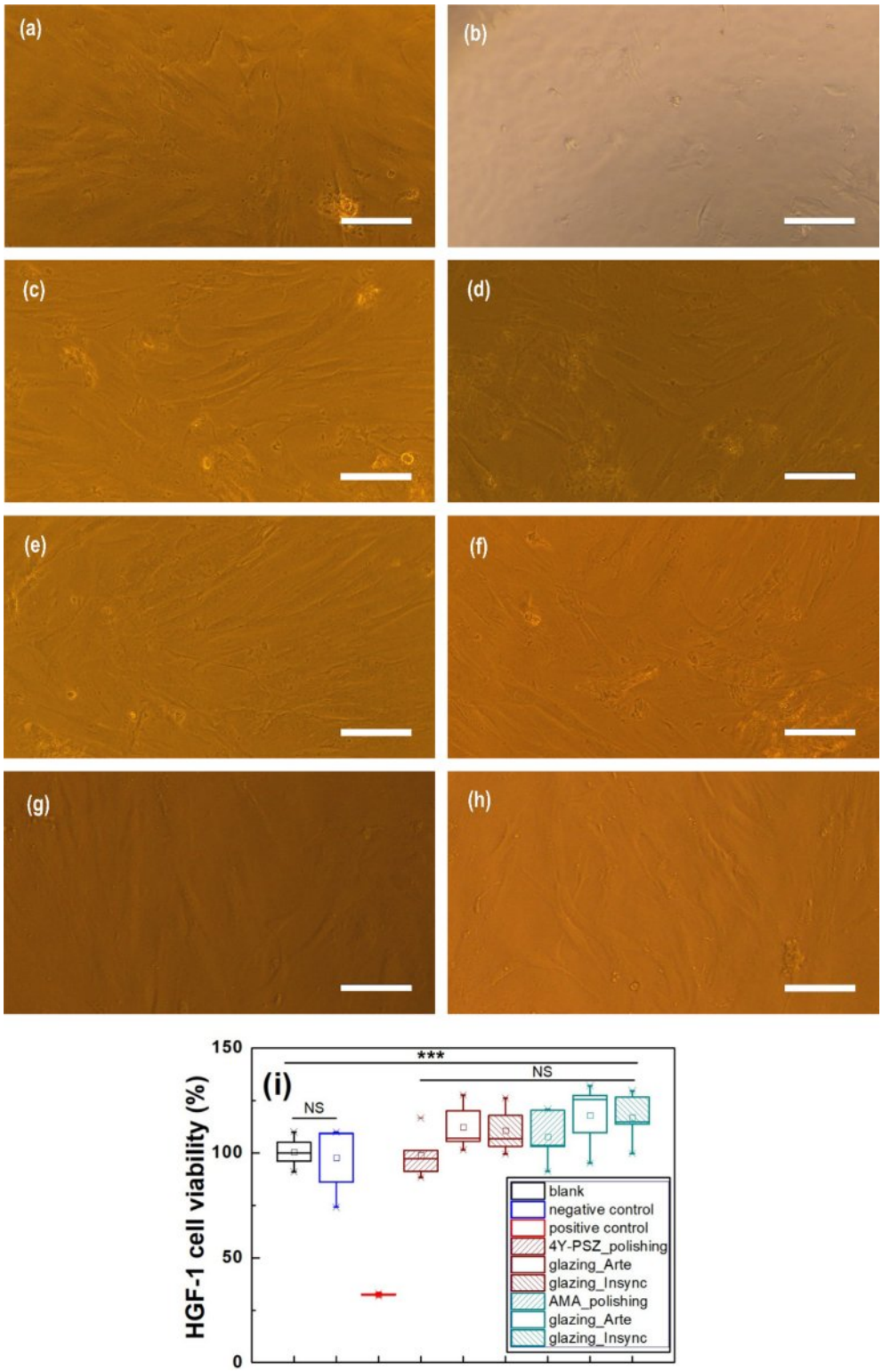

Fig. 5. HGF-1 cell morphology images: (a) negative control, (b) positive control, (c)(f) polished 4Y-PSZ and AMA ceramics, (d)(g) Arte-, (e)(h) Insync-glazed 4Y-PSZ and AMA ceramics, respectively, after 48 h of exposure to suspension in EZ-cytox. (i) Box plot of the HGF-1 cell viability in various samples. Statistical significance is indicated by ***, p < 0.001 (n = 5). NS indicates statistically insignificant. Scale bar is 100 μm.

However, no dramatic difference in the WCA was evident between the Arte and Insync glaze samples ($p = 0.974$).

The cell viability was measured on the 4Y-PSZ and AMA ceramics under various surface conditions. The experimental results were statistically significant ($p < 0.001$). The HGF-1 cell viability was greater than 98% for all samples (Table 2 and Fig. 5). In the positive control (Fig. 5(b)), the HGF-1 cells were round and apoptotic. However, in the negative control (Fig. 5(a)) and the samples, the HGF-1 cells exhibited a typical fibroblastic morphology, with an elongated and spindle-shaped shape. There was no dramatic difference in the HGF-1 cell viability among the various samples ($p > 0.05$). Under the conditions used in this study, no cytotoxicity was evident in any of the samples. This suggests that all samples exhibited excellent cytocompatibility, regardless of the material type or surface treatment.

The HGF-1 cell adhesion and proliferation were further investigated using a live/dead assay kit [11, 18–20]. The viable cells (green staining) and dead cells (red staining) were qualitatively observed using fluorescence microscopy [11, 18–24]. As shown in Fig. 6, the green-stained HGF-1 cells were predominantly observed throughout the samples, with significant cell attachment and growth evident in the glazed samples. The polished 4Y-PSZ exhibited a lower cell density probably owing to its higher WCA [11]. The cell density of the glazed AMA sample increased. Furthermore, the cell density was found to be a strong function of the WCA. A decrease in the highly hydrophilic WCA indicated an increase in the HGF-1 cell density. Overall, the highest cell densities were evident in Arte-glazed 4Y-PSZ and AMA ceramics, as demonstrated in Fig. 6.

Glazes are typically composed of silica, silicon, aluminum oxide, calcium oxide, lithium oxide, or boron oxide, as listed in Table 1 [11, 17, 25, 26]. Hydrophilic silica-rich glazes provides highly hydrophilic surfaces [11, 17]. This treatment is very effective in lessening the adhesion of oral bacteria and impeding biofilm formation on the sample surface. Moreover, glazes can be beneficial for the attachment and growth of HGF-1 cells and is therefore recommended for use in dental prosthetics [25, 26]. Sandblasting prior to glazing has several limitations, including the potential for microcracks that can reduce the mechanical strength of zirconia and the potential for a phase transformation from tetragonal to monoclinic, which can alter properties [17, 27–30]. To overcome these shortcomings, surface modifications such as heat treatment, laser surface texturing, or glazing are necessary [17, 27–31]. Among these, glazed specimens provide a coating layer that fills scratches, cracks, and imperfections that may occur during sandblasting [17, 27–30]. They also offer advantages such as moisture protection, improved mechanical strength, and the elimination of surface defects.

The effectiveness of glazed dental prostheses can be enhanced through cell attachment and growth, and the strength degradation can be deferred by reducing their exposure to oral moisture. Among the surface-treated

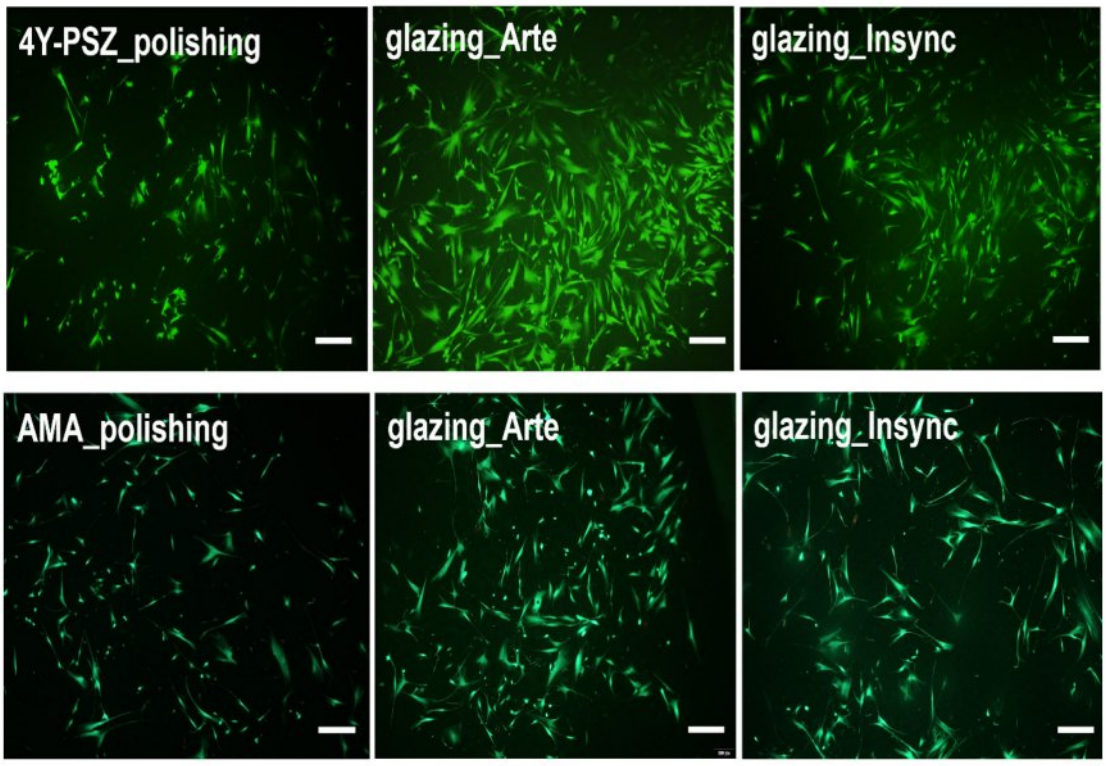

Fig. 6. Live/dead assay of the HGF-1 cells seeded onto various 4Y-PSZ and AMA ceramics. Scale bar is 400 μm.

specimens, the glazed specimens had the lowest WCA and bulk density, suggesting that hydrophilicity was a key factor in cell attachment and growth. Consequently, applying glaze to 4Y-PSZ and AMA ceramics can enhance the cell attachment and growth in dental applications.

The live/dead staining photographs of the bacteria attached to the surfaces of the 4Y-PSZ and AMA specimens are shown in Fig. 7. Lower biofilm biothicknesses were evident on all the glazed specimens compared to the polished specimens. As shown in Fig. 7(c), the biofilm thickness of the Arte-glazed 4Y-PSZ (74.16±2.887 μm) was reduced by 14% compared to that of the polished 4Y-PSZ (85.83±2.887 μm). After Insync glaze treatment, the biofilm thickness of the polished AMA specimens was reduced by 19.5% from 89.25±1.750 μm to 72.33±8.808 μm. However, as shown in Table 2 and Fig. 7(c), there was no statistically significant difference between each group ($p = 0.175$, $n = 5$). The biofilm biothickness was affected by the material type ($\eta_p^2=0.118$, $p = 0.228$), surface treatment ($\eta_p^2=0.633$, $p < 0.01$), and interaction between the material type and surface treatment ($\eta_p^2=0.507$, $p < 0.05$). According to statistical results, the surface treatment was a strong function of the biothickness. Although the bacterial colonization patterns were similar across all samples, there may have been differences in the density of the attached organisms.

The biofilm biomass was then measured for quantitative analysis. There were differences in the bacteria biomass attached to the various sample surfaces. The null hypothesis that surface treatment had no effect on the biofilm biomass of the 4Y-PSZ and AMA ceramics was rejected ($p < 0.05$, $n = 5$). The biomass was affected by

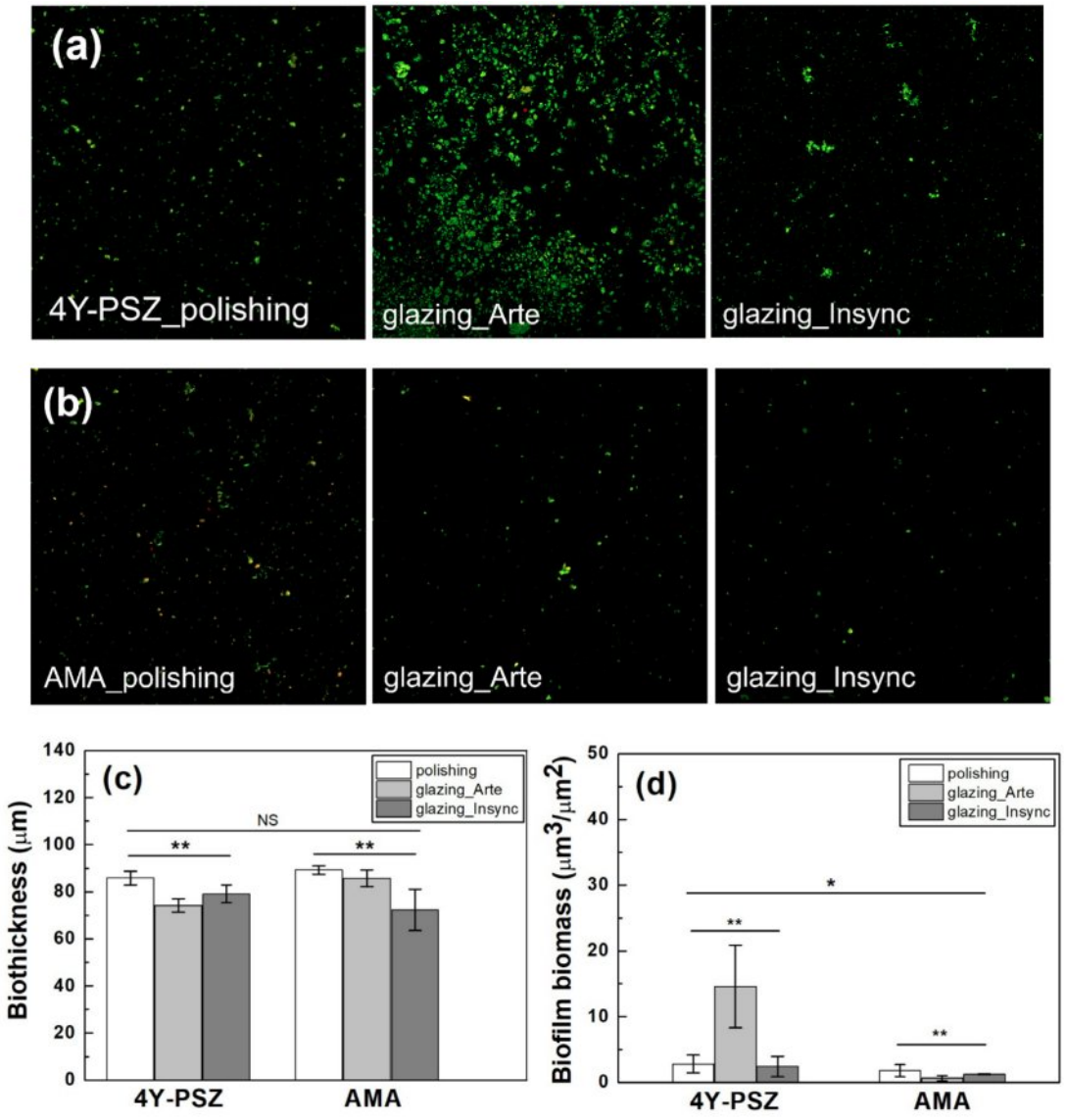

Fig. 7. (a) Live/dead staining images of the bacteria attached to the surfaces of the (a) 4Y-PSZ and (b) AMA specimens. Quantitative analysis of the (b) biothickness and (c) biomass of the biofilms. Statistical significance is indicated by * ($p < 0.05$) and ** ($p < 0.01$, $n = 5$). NS indicates statistically insignificant.

the material type (η_p^2=0.512, $p < 0.01$), surface condition (η_p^2=0.948, $p < 0.001$), and interaction between the material type and surface condition (η_p^2=0.549, $p < 0.01$). The differences in the biomass between the 4Y-PSZ and AMA ceramics were evident. Moreover, the surface condition had a greater effect on the biomass than did the material type.

Kim et al. [22] reported that the biomass of dental ceramic blocks could be reduced by 56% by incorporating up to 0.15wt% of zwitterions (2-methacryloyloxyethy phosphorylcholine and sulfobetain methacrylate in equimolar ratio). However, with increasing zwitterion content, the strength decreased significantly, limiting its widespread use in dental materials. In this study, the highest biofilm biomass value (14.58±6.30 $\mu m^3/\mu m^2$) was observed in the Arte-glazed 4Y-PSZ, which requires further study. The Arte-glazed AMA (0.62±0.384 $\mu m^3/\mu m^2$) exhibited a 65% reduction in biofilm biomass compared to that of the polished AMA (1.775±0.920 $\mu m^3/\mu m^2$). However, the biomass values of the Insync-glazed 4Y-PSZ and AMA ceramics were 2.408±1.556 and 1.233±0.025 $\mu m^3/\mu m^2$, respectively, which were lower than those of the polished 4Y-PSZ (2.793±1.357 $\mu m^3/\mu m^2$) and AMA samples.

Cho et al. [11] reported that the biomass of machined 4Y-PSZ and AMA were 17.019±9.797 and 6.037±0.487 $\mu m^3/\mu m^2$, respectively, suggesting that the biomass of Insync-glazed 4Y-PSZ and Arte-glazed AMA could be reduced by 85.8% and 89.7%, respectively, when considering the machined 4Y-PSZ and AMA as controls. Nonetheless, polishing, although worse than glazing, may improve hydrophilicity compared to machining. It has been reported that glaze treatment reduces bacterial adhesion by lowering surface energy [5,11]. The observed low biomass values indicated a strong opposition to biofilm adhesion, implying that bacterial attachment may be hampered by the formation of a hydration shell on the surface and steric repulsion [5, 11, 17, 32–34]. However, glazing may also promote bacterial attachment to certain materials by increasing the surface voids or inducing localized surface imperfections [11, 32–36]. These dual effects highlights the significance of optimizing the glazing protocol to diminishing undesirable surface characteristics. The surface conditions significantly influenced the biofilm formation on dental ceramics, suggesting that both polishing and glazing can have a beneficial effect on the bacterial resistance. Overall, all polished 4Y-PSZ and AMA samples exhibited excellent bacterial resistance, with bacterial inhibition being even more pronounced after glazing. Clinically, glazing can be considered highly effective for dental restoration applications.

Conclusion

The surface properties, cytocompatibility, and bacterial resistance of polished and glazed 4Y-PSZ and AMA dental ceramics were analyzed as a function of the material type and surface treatment. The effect of the *Ra* on the biological responses of the surface-treated samples was minimal as it was below the roughness threshold. However, Arte and Insync glazing significantly reduced the WCA and bulk density of the 4Y-PSZ and AMA ceramics, thereby improving their surface wettability. Consequently, the glazed surfaces promoted the attachment and proliferation of HGF-1 fibroblasts, suggesting that their superior cytocompatibility enhanced soft tissue adhesion around the dental implants. The Arte-glazed 4Y-PSZ and Insync-glazed AMA specimens exhibited lower biothickness. Furthermore, the Insync-glazed 4Y-PSZ and Arte-glazed AMA samples exhibited lower biomass, indicating improved antibacterial adhesion compared to that of the polished samples. Polishing improved the cell performance and antibiofilm formation, and glazing treatment further enhanced efficacy. Consequently, applying glaze to the dental ceramic surface can significantly prevent peri-implant diseases and improve the prognosis of implant prostheses, regardless of the type of glaze.

Acknowledgements

This work was supported by the Medical Device Development Fund, provided by the Korean government (Ministry of Science and ICT, Ministry of Trade, Industry and Energy, Ministry of Health & Welfare, and Ministry of Food and Drug Safety), the Integrated Life Cycle Medical Device R&D Project (grant number: RS-2023-00255335) supervised by the Integrated R&D Information System (IRIS), the Regional Specialized Industry Development Plus Program (grant number: S3366101) supported by the Ministry of SMEs and Startups (MSS, Republic of Korea), and the Regional Innovation System & Education (RISE) Glocal University 30 Project Program, funded by the Ministry of Education (MOE) and Gangwon State (G.S.), Republic of Korea (2025-RISE-10-004).

References

1. C. Brunot-Gohin, J.L. Duval, S. Verbeke, K. Belanger, I. Pezron, G. Kugel, D. Laurent-Maquin, S. Gangloff, and C. Egles, J. Periodontal Implant Sci. 46 (2016) 362-371.
2. J. Lubauer, R. Belli, H. Peterlik, K. Hurle, and U. Lohbauer, Dent. Mater. 38 (2022) 318-332.
3. A.A. Diken Turksayar, M. Demirel, M.B. Donmez, J. Prosthodont. 32 (2023) 815-820.
4. R. Belli, U. Lohbauer, F. Goetz-Neunhoeffer, and K. Hurle, Dent. Mater. 35 (2019) 1130-1145.
5. C. Brunot-Gohin, J.-L. Duval, E.-E. Azogui, R. Jannetta, I. Pezron, D. Laurent-Maquin, S.C. Gangloff, and C. Egles, Dent. Mater. 29[9] (2013) e205-212.
6. S.E. Doğan, G. Sağlam, M. Acar, and E. Evci, J. Ceram. Proc. Res. 26(4) (2025) 567-572.
7. H.B. Lim, K.-S. Oh, Y.-K. Kim, and D.Y. Lee, Mater. Sci. Eng. A 483 (2008) 297-301.

8. D.J. Kim, M.H. Lee, D.Y. Lee, and J.S. Han, J. Biomed. Mater. Res. 53 (2000) 438-443.
9. K. Tang, M. Luo, W. Zhou, L.-N. Niu, J.-H. Chen, and F. Wang, Bioact. Mater. 27 (2023) 348-361.
10. D.Y. Lee, J. Mater. Sci. 39 (2004) 3141-3145.
11. Y. Cho, M. Cho, J. Ryu, J. Kim, S. Choi, H. Shim, M. Hong, and D.Y. Lee, J. Funct. Biomater. 16[11] (2025) 400.
12. A. Scarano, M. Piattelli, S. Caputi, G.A. Favero, and A. Piattelli, J. Periodontol. 75 (2004) 292-296.
13. L. Rimondini, L. Cerroni, A. Carrassi, and P. Torricelli, Int. J. Oral Maxillofac. Implants 17 (2002) 793-798.
14. S. Wang, Y. Zhao, A.P. Breslawec, T. Liang, Z. Deng, L.L. Kuperman, and Q. Yu, npj Biofilms Microbiomes 9 (2023) 63.
15. H. Nygren, S. Alaeddin, I. Lundström, and K. Magnusson, Biophys. Chem. 49 (1994) 263-272.
16. E. Jerman, N. Lümkemann, M. Eichberger, C. Zoller, S. Nothelfer, A. Kienle, and B. Stawarczyk, Dent. Mater. 37 (2021) 212-222.
17. J. Lee, C. Lee, and J. Song, J. Dent. Hyg. Sci. 17 (2017) 358-367.
18. D.Y. Lee, Int. J. Mol. Sci. 25 (2024) 5022.
19. Y. Cho, H. Jeong, B. Kim, J. Jang, Y. Song, and D.Y. Lee. Polymers 15 (2023) 3844.
20. Y. Jang, J. Jang, B. Kim, Y. Song, and D.Y. Lee, Tissue Eng. Regen. Med. 21 (2024) 557-569.
21. C. Grenade, M. De Pauw-Gillet, P. Gailly A. Vanheusden, and A. Mainjot, Cytotechnology 32 (2016) 2437-2448.
22. M. Kim, J. Mangal, J. Seo, J. Kim, J, Kim, J. Ryu, H. Kim, K. Lee, J. Kwon, and S. Choi, J. Dent. 148 (2024) 105054.
23. J. Ryu, U. Mangal, M. Lee, J. Seo, I.J. Jeong, J. Park, J. Na, K. Lee, H. Yu, J. Cha, J. Kwon, and S. Choi, Biomater. Sci. 11 (2023) 6299-6310.
24. D. Kim, M. Lee, J. Kim, D. Lee, J. Kwon, and S. Choi, Sci. Rep. 9 (2019) 19550.
25. A.J. McBain, C. Sissons, R.G. Ledder, P.K. Sreenivasan, W. De Vizio, and P. Gilbert, J. Appl. Microbiol. 98 (2005) 624-634.
26. F. Wang, T. Yu, and J. Chen, J. Prosthodont. Res. 64 (2020) 71-77.
27. P.C.L. Carvalho, C.C.M.S. Almeida, R.O.A. Souza, and R.N. Tango, Materials 15 (2022) 5449.
28. T.S.A. Haimed, S.J. Alzahrani, E.A. Attar, and L.E. Al-Turki, Materials 16(18) (2023) 6148.
29. M. He, Z. Zhang, D. Zheng, N. Ding, and Y. Liu, Dent. Mater. J. 33 (2014) 778-785.
30. J. Yoon, Prosthesis 7 (2025) 19.
31. M. Tomanik, M. Kobielarz, J. Filipiak, M.Szymonowicz, A. Rusak, K. Mroczkowska, A. Antonczak, and C. Pezowicz, Materials 3 (2020) 3786.
32. S. Veerachamy, T. Yarlagadda, T. Manivasagam, and P.K. Yarlagadda, Proc. Inst. Mech. Eng. H 228 (2014) 1083-1099.
33. L. Hall-Stoodley, J.W. Costerton, and P. Stoodley, Nat. Rev. Microbiol. 2 (2004) 95-108.
34. J.W. Costerton, P. Stewart, and E.P. Greenberg, Science 284 (1999) 1318-1322.
35. F. Murillo-Gómez, F. Murillo-Alvarado, F. Vásquez-Sancho, E. Avendaño, and R. Urcuyo, J. Dent. 148 (2024) 105257.
36. A.M. Fouda, B. Stawarczyk, M. Özcan, L. Singer, and C. Bourauel, J. Mech. Behav. Biomed. Mater. 146 (2023) 106102.